

Spectroscopy of ^{213}At , ^{212}Po , and ^{210}Pb following $^{208}\text{Pb} + ^7\text{Li}$ T. P. Sjoreen,* U. Garg,[†] and D. B. Fossan

Department of Physics, State University of New York, Stony Brook, New York 11794

(Received 9 July 1979)

The bombardment of ^{208}Pb by ^7Li ions has been used to study the properties of excited states in ^{213}At , ^{212}Po , and ^{210}Pb . In-beam measurements with Ge(Li), intrinsic Ge, and Si surface barrier detectors of α -decay excitation functions, α - γ coincidences, γ - γ coincidences, γ -ray angular distributions, and pulsed-beam- γ timing were made to establish decay schemes, level energies, γ -ray multipolarities, spin-parity assignments, and isomeric lifetimes. Excited states with spins up to $19/2 \hbar$ in ^{213}At and $6 \hbar$ in ^{212}Po were identified. The mean lifetimes of the 1272-keV 8^+ and 1193-keV 6^+ states in ^{210}Pb were measured to be 225(22) and 30(10) nsec, respectively. These lifetimes imply $B(E2)$ values of $51(12) e^2 \text{fm}^4$ for the 8^+ state and $308(115) e^2 \text{fm}^4$ for the 6^+ state. The ^{213}At decay scheme and the ^{210}Pb $B(E2)$ values are compared with shell model calculations.

NUCLEAR REACTIONS $^{208}\text{Pb}(^7\text{Li}, 2n)^{213}\text{At}$, $^{208}\text{Pb}(^7\text{Li}, t)^{212}\text{Po}$, $^{208}\text{Pb}(^7\text{Li}, \alpha p)^{210}\text{Pb}$, $E_{\text{Li}} = 30\text{--}34$ MeV; measured α -decay excitations, α - γ coincidences, γ - γ coincidences, γ - $W(\theta)$, pulsed-beam- γ timing; deduced level schemes, γ multipolarities, J^π , $T_{1/2}$, $B(E2)$.

I. INTRODUCTION

The shell model has been very successful in describing the properties of nuclei near the doubly closed ^{208}Pb core ($N = 126$, $Z = 82$). As a result there has been considerable experimental and theoretical interest in this region. For nuclei with $Z > 82$ and $N > 126$, there is a lack of experimental spectroscopic information because it is difficult to populate these nuclei. However, the bombardment of ^{208}Pb by ^7Li has proved to be very useful in studying such nuclei. It has been used to study ^{212}At (Ref. 1) and ^{210}Bi ,² as well as the closed neutron shell ($N = 126$) nuclei of ^{209}Bi (Ref. 3) and ^{211}At .⁴ In the present study, $^7\text{Li} + ^{208}\text{Pb}$ has also been used along with in-beam γ -ray methods to investigate the $N = 128$ nuclei ^{213}At ($Z = 85$), ^{212}Po ($Z = 84$), and ^{210}Pb ($Z = 82$).

The nucleus ^{213}At is composed of five valence particles, three protons and two neutrons, outside of the ^{208}Pb core, while the nucleus ^{212}Po has four valence particles, two protons and two neutrons. The low-lying high-spin states in these nuclei are expected to involve primarily neutrons in the $g_{9/2}$, $i_{11/2}$, and $j_{15/2}$ orbitals and protons in the $h_{9/2}$, $f_{7/2}$, and $i_{13/2}$ orbitals. Spectroscopic information for these nuclei would be useful in the study of the neutron-proton effective interaction. The nucleus ^{210}Pb is somewhat simpler than ^{212}Po and ^{213}At , since it is composed of just two neutrons outside of ^{208}Pb . In this nucleus it would be particularly interesting to acquire lifetime information, which could be used to extract neutron $E2$ effective charges. The purpose of the present study is to experimentally determine the properties of low-

lying high-spin states in ^{213}At , ^{212}Po , and ^{210}Pb and to interpret the results in terms of the shell model.

At the beginning of the present study, the only available information for ^{213}At was the study⁵ of the α decay of the ground state [$T_{1/2} = 110(20)$ nsec], which was observed to decay via a 9.08-MeV α particle to the ^{209}Bi ground state. For ^{212}Po , the available experimental information included studies^{6,7} of the α decay of the ground state [$T_{1/2} = 0.296(2) \mu\text{sec}$] to ^{208}Pb and the β decay of ^{212}Bi to low-spin states ($J \leq 2$) in ^{212}Po . For ^{210}Pb , available experimental information included transfer reaction and β -decay measurements.⁸ With these measurements, many levels in ^{210}Pb were identified, including the 8^+ , 6^+ , 4^+ , 2^+ yrast states.

In the present study, excited states in ^{213}At , ^{212}Po , and ^{210}Pb were populated via the $^{208}\text{Pb}(^7\text{Li}, 2n)$, $^{208}\text{Pb}(^7\text{Li}, t)$, and $^{208}\text{Pb}(^7\text{Li}, \alpha p)$ reactions, respectively. To extract the required information, several in-beam measurements were carried out. α -decay excitation measurements were made to investigate the $(^7\text{Li}, 2n)$ and $(^7\text{Li}, t)$ yields near the Coulomb barrier; an α - γ coincidence measurement was carried out to identify γ rays from ^{213}At and γ - γ coincidence, γ -ray angular distribution, and pulsed-beam- γ timing measurements were made to determine level energies, spin and parity assignments, γ -ray multipolarities, and isomeric lifetimes. The experimental techniques used in the α -decay excitation and α - γ coincidence measurements are described in Sec. II. The techniques for the γ - γ coincidence, γ -ray angular distributions, and pulsed-beam- γ timing measure-

ments are discussed in detail in Ref. 9, and are also briefly reviewed in Sec. II. The experimental results for ^{213}At and ^{210}Pb are presented in Sec. III, and discussed in terms of the shell model in Sec. IV. The ^{212}Po results are presented in Sec. III, and are also compared in Ref. 10 with a complete ^{212}Po shell model calculation. Preliminary results of these measurements have been reported previously.¹¹ An independent study of ^{212}Po employing the $^{208}\text{Bi}(\alpha, p)$ reaction has also been recently performed to investigate high-spin states.¹²

II. EXPERIMENTAL PROCEDURE

Levels in ^{213}At , ^{212}Po , and ^{210}Pb were populated via the $^{208}\text{Pb}(^7\text{Li}, 2n)$, $^{208}\text{Pb}(^7\text{Li}, t)$, and $^{208}\text{Pb}(^7\text{Li}, \alpha p)$ reaction, respectively. For these measurements, 30–34-MeV $^7\text{Li}^{3+}$ beams, obtained from the Stony Brook tandem van de Graff accelerator were incident on enriched (>99%) ^{208}Pb foils with thicknesses of 0.5, 1.1, and 250 mg/cm^2 . The deexcitation γ rays were detected by large coaxial Ge(Li) detectors with energy resolutions of ~ 2.0 keV full width at half maximum (FWHM) at 1.3 MeV. For weak low-energy γ rays (<400 keV), a planar type Ge detector, with an energy resolution of 0.8 keV FWHM at 122 keV, was utilized in several measurements. The α particles were detected by silicon surface barrier detectors, including one of annular geometry, which were typically 150 $\mu\text{g}/\text{cm}^2$ thick and 100–150 mm^2 in area.

The α -decay excitation study was carried out to determine the relative cross sections for the population of ^{212}At , ^{213}At , and ^{212}Po near the $^7\text{Li} + ^{208}\text{Pb}$ Coulomb barrier. This was done by measuring the α -decay yields at ^7Li beam energies of 30, 32, and 34 MeV with the 0.5 mg/cm^2 ^{208}Pb target. The energies of the α -particle groups for these nuclei are 9.08 MeV for ^{213}At ,⁵ 8.78 MeV for ^{212}Po ,⁷ and primarily 7.62, 7.68, 7.84, and 7.90 MeV for ^{212}At .¹³ All other expected α -particle groups have energies less than 7.45 MeV. The α particles were detected at 160° relative to the beam direction with a silicon detector (see Fig. 1). An in-beam resolution of 150 keV FWHM, which was limited by the target thickness, was sufficient to resolve the α -particle groups. The yield for each α -particle group was determined by fitting to the data a Gaussian distribution with a quadratic background. The yield for ^{212}At was obtained by summing the 7.62-, 7.68-, 7.84-, and 7.90-MeV α -particle group yields. Normalization was achieved by current integration. On the basis of these yields, the beam energies for the subsequent $^7\text{Li} + ^{208}\text{Pb}$ measurements were selected.

A coincidence measurement between γ rays and the ground state α decay of ^{213}At was made to

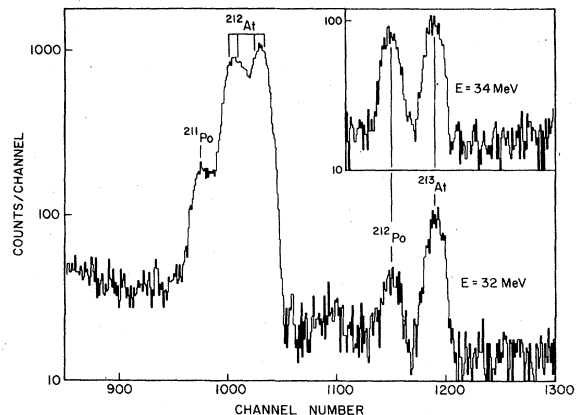


FIG. 1. The α -particle energy spectrum observed with a 0.5 mg/cm^2 ^{208}Pb target at a ^7Li beam energy of 32 MeV. The energies of the α -particle groups are 9.08 MeV for ^{213}At ; 8.78 MeV for ^{212}Po ; primarily 7.62, 7.68, 7.84, and 7.90 MeV for ^{212}At ; and 7.45 MeV for ^{211}Po . The insert in the upper right corner contains the relative yield of the ^{212}Po and ^{213}At groups at 34 MeV.

identify those γ rays originating from the decay of excited states in ^{213}At . Care had to be exercised because of the considerably larger yield of the $(^7\text{Li}, 3n)$ channel to ^{212}At (see Sec. III). In order to achieve a reasonable coincidence event rate for this measurement, large detector solid angles, an optimal ^{213}At yield, and a thick target were required. The large detector solid angles were obtained by using a target chamber which was designed to allow an annular surface barrier detector and a Ge(Li) detector to be placed as close as 3 cm from the target when the detectors are positioned at 180° and 90° to the beam, respectively. The optimal ^{213}At yield was achieved by carrying out the experiment at a 30-MeV beam energy. This energy was selected on the basis of the α -decay excitation measurements, which showed that for the range of energies studied, the yield of ^{213}At was a maximum at 30 MeV and that for ^{212}At was at a minimum. Below 30 MeV the Coulomb barrier reduced all the channels. In addition, since the yield of ^{212}Po at 30 MeV is down by about an order of magnitude relative to that for ^{213}At , it was not necessary to resolve the ^{212}Po and ^{213}At decay α particles, which are separated by only 300 keV. Thus a thick 1.1 mg/cm^2 target could be used to increase the coincidence α - γ event rate for ^{213}At . The α energy resolution with this target thickness was adequate to discriminate against the ^{212}At α groups. For the α - γ coincidence measurement, standard fast-slow electronics were employed; this was possible because the mean lifetime, $\tau = 159(29)$ nsec, of the ^{213}At ground state is sufficiently short that the true-to-random ratio is acceptable. Coincident γ -ray spectra were

collected on-line by setting digital gates on the 9.08-MeV α particles from ^{213}At .

The γ - γ coincidence, γ -ray angular distribution, and pulsed-beam- γ timing measurements were carried out using 33-MeV ^7Li ion beams and the thick 250 mg/cm² target. The increased energy was chosen to increase the population of high-spin states and at this energy the ^{213}At yield relative to ^{212}At is still reasonable. The yield for ^{212}Po is also large enough that spectroscopic information could be obtained. The γ - γ coincidence measurements were carried out to identify the γ -ray decay schemes. To obtain information on the γ -anisotropies, as well as the relative γ -ray intensities I_γ , γ -angular distributions were measured at 5 angles between 0° and 90°. The extracted photo-peak areas were fitted to $W(\theta) = I_\gamma(1 + A_2P_2 + A_4P_4)$, where P_k are the Legendre polynomials. The time differential pulsed-beam- γ measurements were made to identify delayed transitions and to obtain lifetime results for isomeric states. For the time differential measurements, the ^7Li beam was pulsed with repetition periods of 1 and 2 μsec and an overall time resolution of about 8 nsec was achieved with the Ge(Li) detectors.

III. EXPERIMENTAL RESULTS

A. ^{213}At and ^{212}Po

The results of the α -decay excitation measurement (see Fig. 2) show that the $^{208}\text{Pb}(^7\text{Li},3n)^{212}\text{At}$ reaction is much stronger than that of $^{208}\text{Pb}(^7\text{Li},2n)^{213}\text{At}$. These results are consistent with the cross-section estimates which are expected¹⁴ to peak at 41.8 and 29.5 MeV for the $(^7\text{Li},3n)$ and $(^7\text{Li},2n)$ reactions, respectively. The yield of the $(^7\text{Li},2n)$ reaction at its peak energy is significantly limited by the Coulomb barrier (≈ 30 MeV). The measurement also shows that the $^{208}\text{Pb}(^7\text{Li},t)^{212}\text{Po}$ reaction has a strong energy dependence between 30–34 MeV. At 30 MeV this reaction is very weak, but increases rapidly, becoming nearly equal to the $^{208}\text{Pb}(^7\text{Li},2n)^{213}\text{At}$ reaction at 34 MeV. The $(^7\text{Li},t)$ reaction is expected¹⁵ to involve both direct transfer and breakup plus capture processes. Calculations with a standard equilibrium evaporation code¹⁶ indicate that the contributions to the ^{212}Po yield from $(^7\text{Li},p2n)$ should be very small compared to the observed yields. Since these results showed that the yield of ^{213}At was largest at 30 MeV for the range of energies studied and that for ^{212}At and ^{212}Po was a minimum, this energy was chosen for the α - γ coincidence measurement in order to optimize the event rate.

From the α - γ coincidence measurement, the 341-, 387-, 405-, and 725-keV γ rays were assigned to ^{213}At . These four γ rays are seen in the

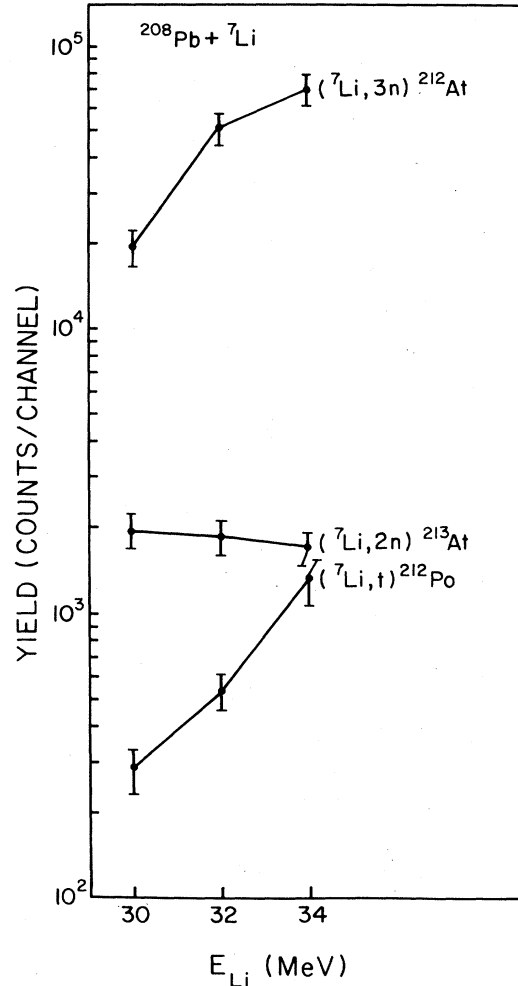


FIG. 2. Relative α -decay yields for ^{212}At , ^{212}Po , and ^{213}At during the bombardment of a 0.5 mg/cm² ^{208}Pb target with ^7Li ions at energies of 30, 32, and 34 MeV. The yield for ^{212}At was obtained by summing the 7.62-, 7.68-, 7.84-, and 7.90-MeV α -particle groups.

coincidence spectrum for the 9.08-MeV α particles of the ground state decay of ^{213}At , which is shown in Fig. 3. The 511-keV γ ray was also observed in coincidence; however, this γ ray is most probably annihilation radiation.

The results of the γ - γ coincidence and angular distribution measurements for ^{213}At and ^{212}Po are summarized in Table I. The 387-, 405-, and 725-keV γ rays assigned to ^{213}At on the basis of the α - γ coincidence measurement are also observed in coincidence with a 188-keV γ ray. These four γ rays are shown in the total γ - γ coincidence spectrum at the top of Fig. 4. The strong γ rays in this spectrum, which are not labeled in the figure, have been identified previously as γ rays from ^{212}At ,¹ ^{210}Bi ,² and ^{209}Bi .³ In addition to the ^{213}At γ rays, γ rays with energies of 727, 405, and 222

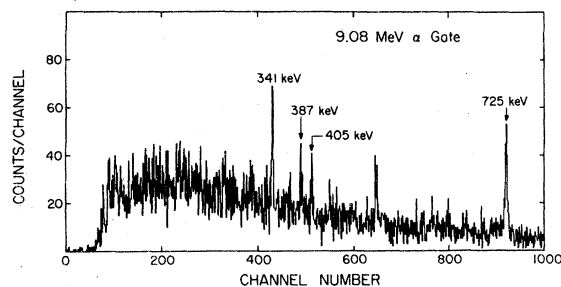


FIG. 3. γ -ray spectrum obtained in coincidence with 9.08-MeV α particles from the decay of the ^{213}At ground state during the bombardment of a 1.1 mg/cm² ^{208}Pb target with 30-MeV ^7Li ions.

keV were assigned to ^{212}Po . This assignment was made with the assumed identification of the 727-keV γ ray with the $2^+ \rightarrow 0^+$ transition in ^{212}Po , which had been observed previously in β -decay studies⁷ of ^{212}Bi . This identification is strengthened by the fact that the ratio of the intensity of the 725-keV transition in ^{213}At to the 727-keV transition (see Table I) is comparable to the ratio of the ^{213}At to ^{212}Po α -decay yields observed at 33 MeV, which is the energy at which the γ - γ coincidence measurements were carried out (see Fig. 2). Also the 727-keV γ ray has not been observed¹⁻³ in coincidence with any of the γ rays from ^{212}At , ^{209}Bi , and ^{210}Bi . Both the ^{213}At and ^{212}Po level schemes involve a 405-keV transition. The existence of two 405-keV γ rays was determined by the γ - γ coincidence measurement which showed that the 725-keV transition in ^{213}At and the 727-keV transition in ^{212}Po were both in coincidence with a 405-keV γ ray (see Fig. 4). Conversely, the 405-keV transition is observed in coincidence with both the 725- and 727-keV γ rays.

From the γ - γ coincidence results and the γ -ray

intensities I_γ , level schemes for ^{213}At and ^{212}Po were constructed. The level scheme for ^{213}At is shown on the left side of Fig. 5. The main feature of the decay scheme is the γ -ray cascade from the 1318-keV level to the ground state involving the 18-, 188-, 387-, 405-, and 725-keV γ rays. The 18-keV transition between the 1130- and 1112-keV levels was not observed, but its existence is confirmed by the coincidence between the 188- and 387-keV γ rays. The 341-keV γ ray is also included in the ^{213}At level scheme, on the basis of the α - γ coincidence measurement. No γ ray was observed in coincidence with this transition, indicating that it decays to the ground state.

For ^{212}Po , the 222- and 405-keV γ rays were observed to cascade to the 727-keV 2^+ state, defining levels at 1132- and 1354-keV (see Fig. 6). The present ^{212}Po results agree with the recent $^{209}\text{Bi}(\alpha, p)^{212}\text{Po}$ study,¹² which observed 727-, 405-, and 222-keV γ rays in coincidence with the ^{212}Po decay α particles. In addition, the present γ - γ coincidence and angular distribution measurements remove any ambiguities in the placement of the 405-, and 222-keV γ rays in the ^{212}Po level scheme.

Evidence for isomerism in both ^{213}At and ^{212}Po was found in the pulsed-beam- γ timing data. All the γ rays listed in Table I had delayed components, except the 341-keV γ ray. The 387-, 405-, 725-, and 727-keV γ rays also showed prompt peaks in their time spectra. Since the 405-keV line is actually two γ rays, it could not be determined definitely whether or not either of the components lacked a prompt peak. However, since both the ^{213}At 188-keV and ^{212}Po 222-keV γ rays are delayed, it is most probable that the 1130-keV level in ^{213}At and the 1132-keV level in ^{212}Po , which

TABLE I. Results of the γ - γ coincidence and angular distribution measurements for ^{212}Po and ^{213}At .

E_γ (keV) ^a	Nucleus	I_γ ^b	A_2 ^c	γ rays coincident with E_γ ^d
188.4	^{213}At	13	-0.21 ± 0.07	(386.7), (405.1), 724.6
221.5	^{212}Po	16	0.05 ± 0.06	405.1, 727.4
340.5	^{213}At	40	0.14 ± 0.04	
386.7	^{213}At	27	-0.35 ± 0.06	188.4, 724.6
405.1	$^{212}\text{Po}, ^{213}\text{At}$	58 ^e	0.21 ± 0.05	188.4, 221.5, 724.6, 727.4
724.6	^{213}At	100	0.28 ± 0.05	188.4, 386.7, 405.1
727.4	^{212}Po	80	-0.01 ± 0.03	221.5, 405.1

^a γ -ray energies are accurate to ± 0.3 keV.

^b γ -ray intensities are normalized to the 724.6-keV yield; intensities are accurate to 10% unless otherwise noted.

^cThe A_4 coefficients are not quoted; all the A_4 coefficients are consistent with 0.00 ± 0.08 .

^dParentheses around γ -ray energy indicate weak coincidence.

^eThe intensities (accurate to 25%) of the ^{213}At and ^{212}Po components of this γ ray are estimated from the γ - γ coincidence measurement to be 33 and 25, respectively.

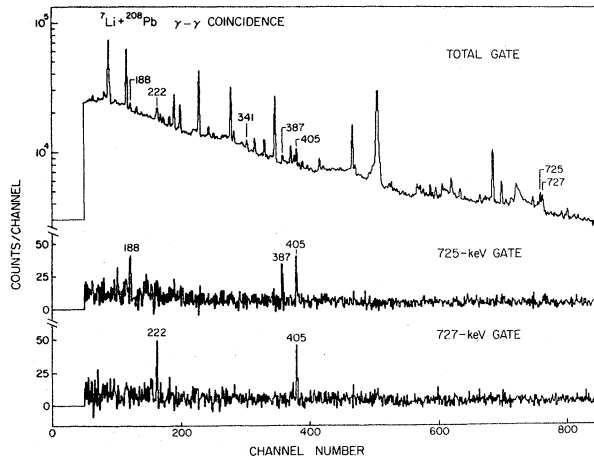


FIG. 4. γ - γ coincidence spectra from the $^{208}\text{Pb} + ^7\text{Li}$ reaction at $E_{\text{Li}} = 33$ MeV. The total gate spectrum is coincident with all γ rays from 50 to 1000 keV. The strong γ rays in this spectrum have been identified previously in $^{208}\text{Pb} + ^7\text{Li}$ studies of ^{212}At (Ref. 1), ^{210}Bi (Ref. 2), and ^{209}Bi (Ref. 3). The 725- and 727-keV gates are from the $(^7\text{Li}, 2n)^{213}\text{At}$ and $(^7\text{Li}, t)^{212}\text{Po}$ reactions, respectively.

decay via the 405-keV γ rays, are not isomeric. From this timing data it was impossible to exclude the existence of prompt components in the 188- and 220-keV γ rays because the prompt Compton background was very large at these energies and the delayed intensity very weak. Based on the above information, isomeric states exist at or above 1318 keV in ^{213}At and 1354 keV in ^{212}Po .

The 387- and 405-keV γ rays were the only transitions from which lifetime information could be extracted. A fit of a single lifetime to the 387-keV time differential data yielded a mean lifetime $\tau = 159(25)$ nsec for the ^{213}At isomer. For the 405-keV transition, which involves two γ rays, the best fit to the time differential spectrum was obtained with a function involving two independent lifetimes, that yielded $\tau = 163(14)$ and $\tau = 25(9)$ nsec. These results suggest that the isomer with the shorter lifetime is in ^{212}Po and that with the longer lifetime in ^{213}At . All the other levels have lifetime upper limits of $\tau \leq 8$ nsec. The observed $\tau = 25$ nsec lifetime in ^{212}Po at or above 1354 keV is consistent with a recent independent $^{209}\text{Bi}(\alpha, p)^{212}\text{Po}$ measurement¹² which identified an isomeric state at 1423(30) keV with a mean lifetime of 20.5(3.5) nsec.

γ -ray multipolarities and, hence, J^π assignments were deduced from the γ -angular distributions with the assumptions that the states are aligned in low- m substates and that the dominant γ -ray decay proceeds via yrast levels by stretched

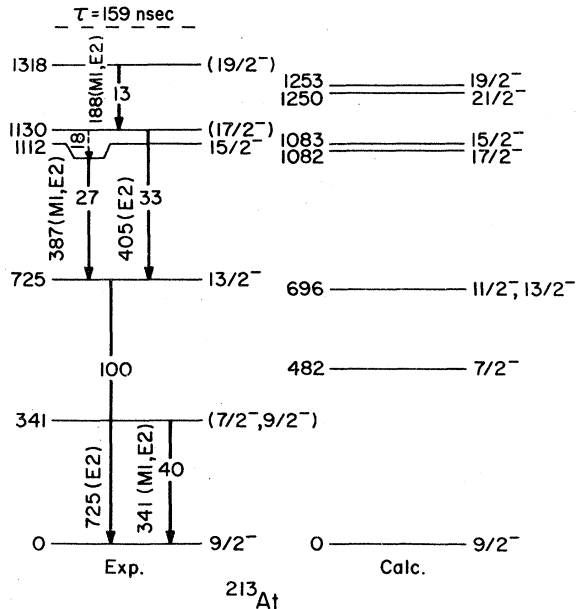


FIG. 5. The experimental and calculated energy level schemes for ^{213}At . The experimental level scheme that was determined from the present $^{208}\text{Pb}(^7\text{Li}, 2n)$ γ -ray measurements is shown on the left side. The energies of the levels and the γ rays are given in units of keV. The γ -ray intensities are normalized to the 725-keV γ -ray yield (=100). The results of the shell model calculation for the $(\pi h_{9/2})^3(\nu g_{9/2})^2$ model space are shown on the right side for several selected levels.

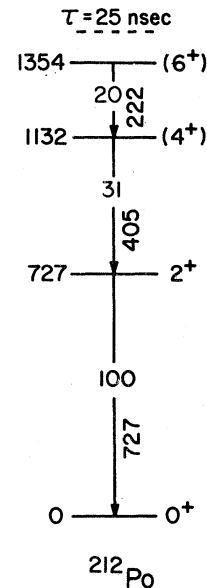


FIG. 6. The energy level scheme for ^{212}Po determined from the present $^{208}\text{Pb}(^7\text{Li}, t)$ γ -ray measurements. The 727-keV $\{2^+ \rightarrow 0^+\}$ transition was taken from Ref. 7.

$J \rightarrow J-L$ transitions,¹⁴ where yrast levels are the lowest energy levels for a given spin J and L is the γ -ray multipolarity. Lifetime information also aided in these assignments by eliminating higher multiplicarities.

The deduced γ -ray multiplicarities and J^π assignments for ^{213}At are included in the level scheme of Fig. 5. Based on the angular distribution coefficients and lifetime limit, the 725-keV γ ray is identified as a stretched $E2$ transition. Assuming $J^\pi = \frac{9}{2}^-$ for the ground state of ^{213}At ,⁵ this multipolarity implies a $J^\pi = \frac{13}{2}^-$ for the 725-keV level. Since there are two 405-keV γ rays, the A_2 and A_4 coefficients for each separate γ ray are uncertain. However, since the angular distributions of the 222- and 727-keV γ rays in ^{212}Po were observed to be isotropic ($A_2 \approx 0$ and $A_4 \approx 0$), the ^{212}Po component of the 405-keV angular distribution is also most likely isotropic. The observed A_K thus suggest that the ^{213}At component for the 405-keV γ ray is a stretched $E2$ transition. This implies a $J^\pi = (\frac{11}{2}^-)$ for the 1130-keV level in ^{213}At ; the bracket denotes the tentative nature of this assignment. For the 387-keV γ ray, the angular distribution and lifetime information strongly suggest a mixed $M1/E2$ multipolarity with a negative mixing ratio. This implies a $J^\pi = \frac{15}{2}^-$ for the 1112-keV level. Similarly, the 188-keV γ ray is consistent with a mixed $M1/E2$ transition. However, the possibility of $E1$ multipolarity cannot be ruled out for this γ ray because of the uncertainty in the A_2 coefficient. Thus, the 1318-keV level is tentatively given an assignment of $(\frac{19}{2}^-)$. For the prompt 341-keV γ ray, the small positive $A_2 = 0.14$ is suggestive of a nonstretched mixed $M1/E2$ transition. The most probable spin and parity for the 341-keV level is $(\frac{7}{2}^-, \frac{9}{2}^-)$.

For the ^{212}Po γ rays, the angular distributions are nearly isotropic (see Table I). However, the 727-keV $2^+ \rightarrow 0^+$ transition is known to be a stretched $E2$. This indicates that the $(^7\text{Li}, t)$ reaction is populating a broad distribution of m sub-states or that dealignment is occurring. Thus, strong J^π assignments cannot be made. However, because ^{212}Po is an even-even nucleus, it is most probable that the yrast decay is proceeding via the usual $6^+ \rightarrow 4^+ \rightarrow 2^+ \rightarrow 0^+$ sequence of levels. For this reason, the 1132- and 1354-keV levels are tentatively given J^π assignments of (4^+) and (6^+) , respectively.

B. ^{210}Pb

The γ - γ coincidence measurements showed that levels in ^{210}Pb were being weakly populated during the bombardment of ^{208}Pb with 33-MeV ^7Li ions. Since the energies of the 8^+ , 6^+ , 4^+ , and 2^+ levels in ^{210}Pb were known from previous charged parti-

cle studies,⁸ the coincidence between the 297- and 799-keV γ rays observed in the present experiment identified these two γ rays as the $4^+ \rightarrow 2^+$ and $2^+ \rightarrow 0^+$ transitions in ^{210}Pb , respectively (see Fig. 7). These ^{210}Pb levels were being weakly populated most probably via the $^{208}\text{Pb}(^7\text{Li}, \alpha p)$ reaction.

Evidence for two isomeric states in ^{210}Pb was found in the time differential data, which showed that both the 297- and 799-keV γ rays had delayed components. The results of the time differential measurement of the 297-keV γ ray are shown in Fig. 7. A least-squares fit to the data yielded mean lifetimes of 225(22) nsec and 30(10) nsec. The time differential spectrum of the 799-keV γ ray, which had poor statistics, also yielded lifetimes consistent with these values. Since the time differential spectra of both γ rays also include prompt components, they indicated that the isomeric levels lie above the 1096-keV 4^+ level and decay most probably via unobserved highly converted transitions. This assumption is consistent with the $8^+ \rightarrow 6^+$ and $6^+ \rightarrow 4^+$ transition energies in ^{210}Pb , which are known⁸ to be 79- and 99-keV, respectively. Such $E2$ transitions have internal conversion coefficients of about 23 and 8, respectively, and would not be observed in the present γ -ray measurements. Thus, the present experimental data suggests that ^{210}Pb is similar to ^{210}Po , where the 8^+ and 6^+ states are known¹⁷ to be isomeric with mean lifetimes of 139 and 61 nsec, respectively. Assuming the same situa-

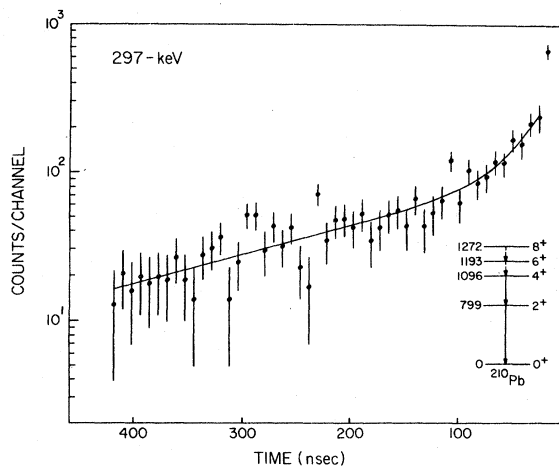


FIG. 7. Results of the time differential measurement of the 1272-keV 8^+ and 1193-keV 6^+ states in ^{210}Pb obtained from the time spectrum of the 297-keV γ ray for the bombardment of a thick ^{208}Pb target with a pulsed 33-MeV ^7Li beam. The solid line is a least squares fit to the data which yielded mean lifetimes of 225(22) and 30(10) nsec. The assignment of these lifetimes to the 8^+ and 6^+ states, respectively in ^{210}Pb is discussed in the text.

tion in ^{210}Pb implies that the 8^+ and 6^+ states have mean lifetimes of 225 and 30 nsec, respectively.

The decay of the recently discovered³ 2986-keV $\frac{19}{2}^+$ isomeric state in ^{209}Bi was also observed in the present experiment. This level was strongly populated via the $^{208}\text{Pb}(^7\text{Li}, \alpha 2n)$ reaction. From the time differential measurements, the mean lifetime of this state was determined to be $\tau = 25(2)$ nsec, which is in excellent agreement with the previously measured value of $\tau = 26.0 \pm 1.4$ nsec.³ The observed decay scheme for this isomer also agrees with that of Ref. 3.

IV. DISCUSSION

^{213}At

The experimental results obtained for ^{213}At from the present $^{208}\text{Pb}(^7\text{Li}, 2n)$ γ -ray measurements are summarized in Table I and on the left side of Fig. 5. The structure of the low-lying states is expected to involve primarily the $h_{9/2}$ protons and the $g_{9/2}$ neutrons. Comparison of the ^{213}At level scheme with those for ^{211}At and ^{210}Pb suggests that the observed states in ^{213}At can be described reasonably well as the $(\pi)^3$ yrast levels in ^{211}At coupled to the $(\nu)^2$ levels of ^{210}Pb .

To check this, a shell model calculation of the energies of the $(\pi h_{9/2})^3(\nu g_{9/2})^2$ structure was made using two-body empirical matrix elements extracted from ^{210}Pb , ^{210}Bi , and ^{211}At .¹⁸ The results of the calculation for the yrast levels $J^\pi = \frac{7}{2}^-, \dots, \frac{21}{2}^-$ are shown on the right side of Fig. 5, where they are compared with the experimental level scheme. The agreement is good. All the calculated levels are within 65 keV of the experimental levels, except for the 341-keV level, which is 142 keV below the calculated $\frac{7}{2}^-$ state. This indicates that, except for the 341-keV level, the observed levels in ^{213}At dominantly involve the $(\pi h_{9/2})^3(\nu g_{9/2})^2$ structure. Furthermore, the calculation shows that the configurations for these levels are primarily the ^{211}At ground state coupled to the $(\nu g_{9/2})^2$ excitations in ^{210}Pb .

In regard to the 341-keV $(\frac{7}{2}^-, \frac{9}{2}^-)$ level, no $\frac{7}{2}^-$ or $\frac{9}{2}^-$ levels are predicted near this energy by the calculation for the $(\pi h_{9/2})^3(\nu g_{9/2})^2$ configuration. This suggests that the 341-keV wave function involves additional orbitals. The orbital most likely involved is $\pi f_{7/2}$ through the

$$|(\pi h_{9/2})^2 0^+(\pi f_{7/2}) \frac{7}{2}^-, (\nu g_{9/2})^2 0^+; \frac{7}{2}^- \rangle$$

configuration. This is supported by ^{211}Bi , where the first excited state, known¹⁹ to have a large component of $|(\pi f_{7/2}), (\nu g_{9/2})^2 0^+; \frac{7}{2}^- \rangle$, is at 410 keV. This energy is considerably lower than the lowest $|(\pi h_{9/2}), (\nu g_{9/2})^2; \frac{7}{2}^- \rangle$ level in ^{211}Bi observed at 765 keV.²⁰

It is interesting to conjecture as to the nature of the $\tau = 159$ nsec isomeric state in ^{213}At . Based on the $(\pi h_{9/2})^3(\nu g_{9/2})^2$ calculation and the experimental information, it is possible that the $|(\pi h_{9/2})^3 \frac{9}{2}^-, (\nu g_{9/2})^2 8^+; \frac{25}{2}^- \rangle$ state would be isomeric, decaying via an unobserved low-energy $E2$ transition ($20 < E_\gamma < 100$ keV) to the $|(\pi h_{9/2})^3 \frac{9}{2}^-, (\nu g_{9/2})^2 6^+; \frac{21}{2}^- \rangle$ state. This $\frac{21}{2}^-$ level would then decay promptly ($\tau \leq 8$ nsec) to the observed $(\frac{19}{2}^-)$ level at 1318 keV by an unobserved low-energy $E1$ transition. According to the $(\pi h_{9/2})^3(\nu g_{9/2})^2$ calculation, the unobserved $\frac{25}{2}^- \rightarrow \frac{21}{2}^-$ $E2$ transition should have an energy of about 60 keV. The isomeric mean lifetime, $\tau = 159$ nsec, then implies a $B(E2) \approx 76 e^2 \text{fm}^4$ using an internal conversion coefficient ≈ 86 . To zeroth order, this $B(E2)$ value should be identical to that for the $8^+ \rightarrow 6^+$ transition of the $(\nu g_{9/2})^2$ neutrons in ^{210}Pb . This value, which is discussed below, is $51(12) e^2 \text{fm}^4$ and is somewhat smaller than that suggested for the $\frac{25}{2}^- \rightarrow \frac{21}{2}^-$ $E2$ transition in ^{213}At .

^{212}Po

The results of the $^{208}\text{Pb}(^7\text{Li}, t)^{212}\text{Po}$ measurements are summarized in Fig. 6 and Table I. These results are compared in a previous paper¹⁰ by D. Strottman with a ^{212}Po shell model calculation, which uses realistic matrix elements and a complete shell model space.

^{210}Pb

The results of the ^{210}Pb lifetime measurements are summarized in Table II. In the present experimental investigation mean lifetimes of 225(22) and 30(10) nsec have been measured in ^{210}Pb for unobserved levels above 1096 keV. Based on the arguments described in Sec. III, these lifetimes were assigned to the 1272-keV 8^+ and 1193-keV 6^+ states, respectively. With these lifetimes, the extracted $B(E2)$ values are $51(12) e^2 \text{fm}^4$ for the $8^+ \rightarrow 6^+$ transition and $308(115) e^2 \text{fm}^4$ for the $6^+ \rightarrow 4^+$ transition.

The results of a calculation of the effective neutron charges in ^{210}Pb are also included in Table II. Theoretical $B(E2)$ values were calculated using the wave functions of Kuo and Herling²¹ and harmonic oscillator radial wave functions with $\hbar\omega = 41A^{-1/3}$. The calculation yielded $B(E2)$ values of $48 e^2 \text{fm}^4$ for $8^+ \rightarrow 6^+$ transition and $187 e^2 \text{fm}^4$ for the $6^+ \rightarrow 4^+$ transition; these values imply neutron effective charges of $1.03(12)e$ and $1.28(24)e$, respectively.

It is interesting to compare the neutron effective charges of ^{210}Pb with those extracted from ^{210}Bi .²² In ^{210}Bi , neutron effective charges of $0.81(8)$ and $0.89(16)$ were obtained from the 9^-

TABLE II. Neutron transitions and effective charges involving the $\nu(2g_{9/2})$ orbitals.

Nucleus	$J_i \rightarrow J_f$	E_γ (keV)	τ (nsec)	α	$B_{\text{exp}}(E2)$ $e^2 \text{fm}^4$	$B_{\text{th}}(E2)$ $e_{\text{eff}}^2 \text{fm}^4$	e_{eff}/e
^{210}Pb	$8^+ \rightarrow 6^+$	$79 \pm 7^{\text{a}}$	225 ± 22	22.3^{b}	51 ± 12	48	1.03 ± 0.12
^{210}Pb	$6^+ \rightarrow 4^+$	$99 \pm 7^{\text{a}}$	30 ± 10	8.3^{b}	308 ± 115	187	1.28 ± 0.24
$^{210}\text{Bi}^{\text{c}}$	$9^- \rightarrow 7^-$	162.3	84 ± 9	0.98	44 ± 5		0.81 ± 0.08
$^{210}\text{Bi}^{\text{c}}$	$5^- \rightarrow 3^-$	90.4	55 ± 9	10.4	190 ± 30		0.89 ± 0.16

^aThe transition energy was taken from Ref. 8.

^bThe internal conversion coefficients were taken from R. S. Hager and C. E. Seltzer, Nucl. Data A4, 1 (1968) and O. Dragoun, Z. Plajner, and F. Schmatzler, *ibid.* A9, 119 (1971).

^cReference 21.

$\rightarrow 7^-$ and $5^- \rightarrow 3^-$ $E2$ transitions, respectively.

Since the dominant configuration for these levels is $|\pi h_{9/2}(\nu g_{9/2})J\rangle$, an effective proton charge of $1.53e$ was used in order to extract the $\nu g_{9/2}$ effective charge. The ^{210}Bi values are slightly smaller than the present ^{210}Pb values, although almost consistent within the uncertainties.

ACKNOWLEDGMENTS

The authors acknowledge Dr. B. A. Brown for contributions which aided in the theoretical interpretation of the experimental results. This study was supported in part by the National Science Foundation.

*Present address: Indiana University Cyclotron Facility, Bloomington, Ind. 47405.

†Present address: Cyclotron Institute, Texas A & M University, College Station, Tex. 77843.

¹T. P. Sjoreen, U. Garg, D. B. Fossan, J. R. Beene, T. K. Alexander, E. D. Earle, O. Häusser, and A. B. McDonald, Phys. Rev. C 20, 960 (1979).

²C. V. K. Baba, T. Faestermann, D. B. Fossan, and D. Proetel, Phys. Rev. Lett. 29, 496 (1972).

³J. R. Beene, O. Häusser, T. K. Alexander, and A. B. McDonald, Phys. Rev. C 17, 1359 (1978).

⁴K. H. Maier, J. R. Leigh, F. Puhlhofer, and R. M. Diamond, Phys. Lett. 35B, 401 (1971).

⁵Jörn Borggreen, Kalevi Valli, and Earl K. Hyde, Phys. Rev. C 2, 1841 (1970).

⁶Suvra Sangul, R. K. Garg, S. D. Chauhan, S. L. Gupta, and S. C. Pancholi, Phys. Rev. C 12, 318 (1975).

⁷S. C. Pancholi and M. J. Martin, Nucl. Data B8, 165 (1972).

⁸E. R. Flynn, G. J. Igo, R. A. Broglia, S. Landowne, V. Paar, and B. Nilsson, Nucl. Phys. A195, 97 (1972), and references therein; E. R. Flynn (private communication).

⁹T. P. Sjoreen, G. Schatz, S. K. Bhattacharjee, B. A. Brown, D. B. Fossan, and P. M. S. Lesser, Phys. Rev. C 14, 1023 (1976).

¹⁰D. Strottman, Phys. Rev. C 20, 1150 (1979).

¹¹T. P. Sjoreen, U. Garg, and D. B. Fossan, Bull. Am.

Phys. Soc. 22, 643 (1977).

¹²R. M. Lieder, J. P. Didelez, H. Beuscher, D. R. Haenni, M. Müller-Veggian, A. Neskakis, and C. Mayer-Böricke, Phys. Rev. Lett. 41, 742 (1978).

¹³Paul L. Reeder, Phys. Rev. C 1, 721 (1970); W. B. Jones, Phys. Rev. 130, 2042 (1963).

¹⁴J. O. Newton, in *Nuclear Spectroscopy and Reactions, Part C*, edited by J. Cerny (Academic, New York, 1974), p. 185.

¹⁵H. Freiesleben, H. C. Britt, J. Birkelund, and J. R. Huizenga, Phys. Rev. C 10, 245 (1974).

¹⁶M. Blam, Code ALICE, U.S.A.E.C. Report No. COO-3494-29 (unpublished).

¹⁷O. Häusser, T. K. Alexander, J. R. Beene, E. D. Earle, A. B. McDonald, F. C. Khanna, and I. S. Townner, Nucl. Phys. A273, 253 (1976).

¹⁸J. P. Schiffer and W. W. True, Rev. Mod. Phys. 48, 191 (1976).

¹⁹E. R. Flynn, R. E. Anderson, N. J. DiGiacomo, R. J. Peterson, and G. R. Smith, Phys. Rev. C 16, 139 (1977).

²⁰E. R. Flynn, D. G. Burke, J. D. Sherman, and J. W. Sunier, Nucl. Phys. A263, 365 (1976).

²¹T. T. S. Kuo and G. H. Herling, NRL Memorandum Report No. 2258, 1971 (unpublished).

²²G. Astner, I. Bergström, J. Blomqvist, B. Fant, and K. Wikström, Nucl. Phys. A182, 219 (1972).